

Passively mode-locked Tm,Ho:YAG laser at 2 μm based on saturable absorption of intersubband transitions in quantum wells

Kejian Yang^{1,2*}, Hubertus Bromberger¹, Hartmut Ruf¹, Hanjo Schäfer¹, Joerg Neuhaus¹, Thomas Dekorsy¹, Christiana Villas-Boas Grimm³, Manfred Helm³, Klaus Biermann⁴, and Harald Künzel⁴

¹Department of Physics and Center of Applied Photonics, University of Konstanz, 78457 Konstanz, Germany

²School of Information Science and Engineering, Shandong University, 250100, China

³Forschungszentrum Dresden-Rossendorf, P.O. Box 510119, 01314 Dresden, Germany

⁴Fraunhofer Institute for Telecommunications (Heinrich Hertz Institut), 10587 Berlin, Germany

*k.j.yang@sdu.edu.cn

Abstract: We report the first demonstration of a solid state laser passively mode-locked through the saturable absorption of short-wavelength intersubband transitions in doped quantum wells: a continuous wave Ti:sapphire laser end-pumped Tm,Ho:YAG laser at the center wavelength of 2.091 μm utilizing intersubband transitions in narrow In_{0.53}Ga_{0.47}As/Al_{0.53}As_{0.47}Sb quantum wells. Stable passive mode-locking operation with maximum average output power of up to 160 mW for 2.9 W of the absorbed pump power could last for hours without external interruption and a mode-locked pulse with duration of 60 ps at repetition rate of 106.5 MHz was generated.

©2010 Optical Society of America

OCIS codes: (140.3070) Infrared and far-infrared lasers; (140.4050) Mode-locked lasers; (140.5680) Rare earth and transition metal solid-state lasers; (140.7090) Ultrafast lasers; (160.6000) Semiconductor, including MQW; (160.4330) Nonlinear optical materials.

References and links

1. T. M. Taczak, and D. K. Killinger, "Development of a Tunable, Narrow-Linewidth, CW 2.066- μm Ho:YLF Laser for Remote Sensing of Atmospheric CO(2) and H(2)O," *Appl. Opt.* **37**(36), 8460–8476 (1998).
2. P. A. Budni, L. A. Pomeranz, M. L. Lemons, C. A. Miller, J. R. Mosto, and E. P. Chicklis, "Efficient mid-infrared laser using 1.9- μm pumped Ho:YAG and ZnGeP₂ optical parametric oscillators," *J. Opt. Soc. Am. B* **17**(5), 723–728 (2000).
3. J. F. Pinto, L. Esterowitz, and G. H. Rosenblatt, "Continuous-wave mode-locked 2- μm Tm: YAG laser," *Opt. Lett.* **17**(10), 731–732 (1992).
4. F. Heine, E. Heumann, G. Huber, and K. L. Schepler, "Mode locking of room-temperature cw thulium and holmium lasers," *Appl. Phys. Lett.* **60**(10), 1161–1163 (1992).
5. G. Galzerano, M. Marano, S. Longhi, E. Sani, A. Toncelli, M. Tonelli, and P. Laporta, "Sub-100-ps amplitude-modulation mode-locked Tm–Ho:BaY₂F₈ laser at 2.06 μm ," *Opt. Lett.* **28**(21), 2085–2087 (2003).
6. D. Gatti, G. Galzerano, A. Toncelli, M. Tonelli, and P. Laporta, "Actively mode-locked Tm–Ho:LiYF₄ and Tm–Ho:BaY₂F₈ lasers," *Appl. Phys. B* **86**(2), 269–273 (2007).
7. U. Keller, "Recent developments in compact ultrafast lasers," *Nature* **424**(6950), 831–838 (2003).
8. F. Haxsen, A. Ruehl, M. Engelbrecht, D. Wandt, U. Morgner, and D. Kracht, "Stretched-pulse operation of a thulium-doped fiber laser," *Opt. Express* **16**(25), 20471–20476 (2008).
9. R. C. Sharp, D. E. Spock, N. Pan, and J. Elliot, "190-fs passively mode-locked thulium fiber laser with a low threshold," *Opt. Lett.* **21**(12), 881–883 (1996).
10. S. Kivistö, T. Hakulinen, M. Guina, and O. G. Okhotnikov, "Tunable Raman Soliton Source Using Mode-Locked Tm–Ho Fiber Laser," *IEEE Photon. Technol. Lett.* **19**(12), 934–936 (2007).
11. Q. Wang, J. Geng, T. Luo, and S. Jiang, "Mode-locked 2 μm laser with highly thulium-doped silicate fiber," *Opt. Lett.* **34**(23), 3616–3618 (2009).
12. A. A. Lagatsky, F. Fusari, S. Calvez, J. A. Gupta, V. E. Kisel, N. V. Kuleshov, C. T. A. Brown, M. D. Dawson, and W. Sibbett, "Passive mode locking of a Tm,Ho:KY(WO₄)₂ laser around 2 μm ," *Opt. Lett.* **34**(17), 2587–2589 (2009).
13. M. A. Solodyankin, E. D. Obraztsova, A. S. Lobach, A. I. Chernov, A. V. Tausenev, V. I. Konov, and E. M. Dianov, "Mode-locked 1.93 microm thulium fiber laser with a carbon nanotube absorber," *Opt. Lett.* **33**(12), 1336–1338 (2008).

14. W. B. Cho, A. Schmidt, J. H. Yim, S. Y. Choi, S. Lee, F. Rotermund, U. Griebner, G. Steinmeyer, V. Petrov, X. Mateos, M. C. Pujol, J. J. Carvajal, M. Aguiló, and F. Dfáz, "Passive mode-locking of a Tm-doped bulk laser near 2 microm using a carbon nanotube saturable absorber," *Opt. Express* **17**(13), 11007–11012 (2009).
15. I. A. Denisov, N. A. Skoptsov, M. S. Gaponenko, A. M. Malyarevich, K. V. Yumashev, and A. A. Lipovskii, "Passive mode locking of 2.09 μm Cr,Tm,Ho:Y₃Sc₂Al₃O₁₂ laser using PbS quantum-dot-doped glass," *Opt. Lett.* **34**(21), 3403–3405 (2009).
16. K. Seeger, *Semiconductor Physics*, 9th edition, Springer, Berlin, 2004.
17. T. Akiyama, N. Georgiev, T. Mozume, H. Yoshida, A. V. Gopal, and O. Wada, "1.55- μm picosecond all-optical switching by using intersubband absorption in InGaAs-AlAs-AlAsSb coupled quantum wells," *IEEE Photon. Technol. Lett.* **14**(4), 495–497 (2002).
18. N. Georgiev, T. Dekorsy, F. Eichhorn, M. Helm, M. Semtsiv, and W. T. Masselink, "Short-wavelength intersubband absorption in strain compensated InGaAs/AlAs quantum well structures grown on InP," *Appl. Phys. Lett.* **83**(2), 210–213 (2003).
19. C. V.-B. Tribuzy, S. Ohser, S. Winnerl, J. Grenzer, H. Schneider, M. Helm, J. Neuhaus, T. Dekorsy, K. Biermann, and H. Künzel, "Femtosecond pump-probe spectroscopy of intersubband relaxation dynamics in narrow InGaAs/AlAsSb quantum well structures," *Appl. Phys. Lett.* **89**(17), 171104 (2006).
20. F. Shohda, M. Nakazawa, R. Akimoto, and H. Ishikawa, "An 88 fs fiber soliton laser using a quantum well saturable absorber with an ultrafast intersubband transition," *Opt. Express* **17**(25), 22499–22504 (2009).
21. C. V.-B. Tribuzy, S. Ohser, M. Priegnitz, S. Winnerl, H. Schneider, M. Helm, J. Neuhaus, T. Dekorsy, K. Biermann, and H. Künzel, "Inefficiency of intervalley transfer in narrow InGaAs/AlAsSb quantum wells," *Phys. Status Solidi* **5**(1), 229–231 (2008) (c).
22. R. C. Stoneman, and L. Esterowitz, "Efficient 1.94- μm Tm:YALO laser," *IEEE J. Sel. Top. Quantum Electron.* **1**(1), 78–81 (1995).
23. A. A. Lagatsky, F. Fusari, S. Calvez, S. V. Kurilchik, V. E. Kisel, N. V. Kuleshov, M. D. Dawson, C. T. A. Brown, and W. Sibbett, "Femtosecond pulse operation of a Tm,Ho-codoped crystalline laser near 2 microm," *Opt. Lett.* **35**(2), 172–174 (2010).
24. L. Zhang, M. Lei, Y. Wang, J. Li, Y. Wang, and J. Liu, "Crystal growth and spectral properties of Yb³⁺:KY(WO₄)₂," *J. Rare Earths* **24**(1), 125–128 (2006).
25. B. Zhou, Z. Wei, Y. Zhang, X. Zhong, H. Teng, L. Zheng, L. Su, and J. Xu, "Generation of 210 fs laser pulses at 1093 nm by a self-starting mode-locked Yb:GYSO laser," *Opt. Lett.* **34**(1), 31–33 (2009).

1. Introduction

Ultrafast lasers emitting in the 2 μm eye-safe region are promising candidates for various applications in coherent doppler wind detection LIDAR, laser ranging, time-resolved spectroscopy, frequency metrology, medicine, optical communication as well as pumping of optical parametric oscillators (OPOs) et al [1,2]. By using active mode-locking approach, picosecond pulses around 2 μm have been obtained in Tm-doped and Tm,Ho-co-doped bulk lasers with host crystals such as Tm:YAG [3], Cr,Tm,Ho:YAG [4], Tm,Ho:BaY₂F₈ [5] and Tm,Ho:LiYF₄ [6]. Compared with active mode-locking, passive mode locking can generate much shorter pulse especially when the saturable absorber is used as mode lockers, besides the virtues of simplicity, compactness and reliability [7]. Up to now, picosecond and femtosecond pulses around 2 μm have been successfully demonstrated in Tm-doped or Tm,Ho-co-doped fiber and bulk lasers based on additive pulse mode-locking [8], saturable absorption mode locking in strained InGaAs multiple quantum wells (MQWs) [9] and Sb-based semiconductor saturable absorber mirrors (SESAMs) [10–12] as well as single wall carbon nanotube [13,14] and PbS quantum dots doped glass [15]. Since additive pulse mode-locking increases the complexity of the laser cavity, the long-term stability of single wall carbon nanotube needs to be further evaluated and PbS quantum-dot-doped glass can still not realize continuous wave mode-locking at 2 μm until now, SESAMs remain a good way to realize mode-locking of fiber or solid-state lasers at 2 μm . However, in the wavelength range of mid-infrared, SESAMs exhibit the problem of a large thermally excited carrier concentration in the conduction band at room temperature, which gives rise to free-carrier absorption of electrons and holes and may induce mode-locking instabilities [16].

Due to the broad flexibility in tuning the absorption strength, the resonance wavelength and the bandwidth by quantum mechanical design, intersubband transitions (ISBTs) in doped semiconductor quantum wells (QWs) have attracted much attention over the past decade and been involved in several mid-infrared optoelectronics devices such as quantum cascade lasers, detectors, and optical modulators [17]. With the advent of the strained QWs structure with large conduction band offset in the conduction band, such as III-V material systems InGaAs/AlAs [18] and InGaAs/AlAsSb [19], intersubband transitions at shorter wavelengths

than 2 μm have been demonstrated. Very recently by using an II-VI semiconductor-based ISBT device, a 1.5 μm passively mode-locked femtosecond fiber laser was successfully demonstrated [20]. Inherently, ISBTs offer ultrafast relaxation dynamics due to the ultrafast nonradiative phonon-assisted relaxation between different subbands on ps to sub-ps time scale. Recently femtosecond pump-probe measurements on narrow InGaAs/AlAsSb QWs with the peak absorption around 2 μm an ISBT relaxation time of 1.2 ps has been observed [21], which shows exciting potential for mode-locking based on saturable absorption at this wavelength.

Here we report a Ti-sapphire laser end-pumped $\text{Tm}^{3+}, \text{Ho}^{3+}$:YAG laser at the center wavelength of 2.091 μm utilizing ISBTs in doped $\text{In}_{0.53}\text{Ga}_{0.47}\text{As}/\text{Al}_{0.53}\text{As}_{0.47}\text{Sb}$ multiple quantum wells grown on an InP substrate - to the best of our knowledge - for the first time. Passive mode-locking operation has been obtained with an average output power of up to 160 mW at a repetition rate of 106.5 MHz, which is stable for several hours.

2. Intersubband absorption in quantum wells

A sequence of 50 QWs in the materials systems $\text{In}_{0.53}\text{Ga}_{0.47}\text{As}/\text{Al}_{0.53}\text{As}_{0.47}\text{Sb}$ was grown lattice matched to double side polished InP:Fe substrate by molecular beam epitaxy (MBE) at 480°C. The full structure is shown as inset in Fig. 1.

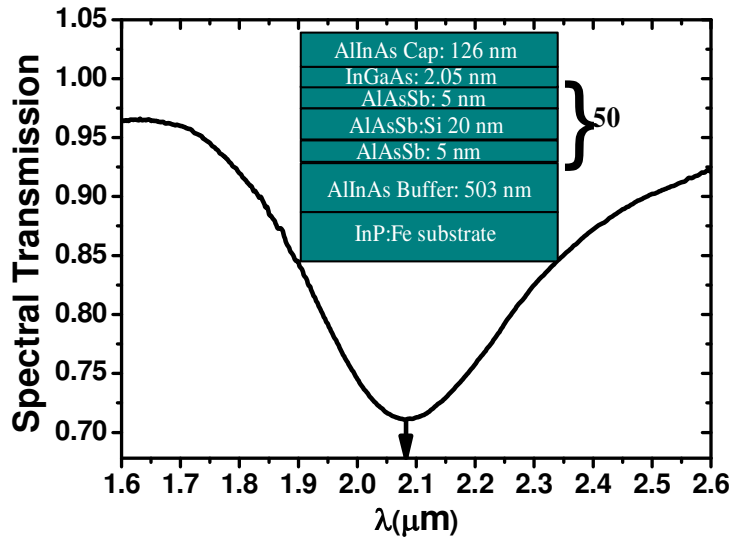


Fig. 1. Static transmission spectrum of $\text{In}_{0.53}\text{Ga}_{0.47}\text{As}/\text{Al}_{0.53}\text{As}_{0.47}\text{Sb}$ MQWs. Inset: Growth structure of $\text{In}_{0.53}\text{Ga}_{0.47}\text{As}/\text{Al}_{0.53}\text{As}_{0.47}\text{Sb}$ MQWs

The nominal InGaAs well width is 2.05 nm and high resolution x-ray diffraction and reflection measurements yielded actual QW thickness of 2.28 nm. The sample is modulation doped in the center of the 20 nm thick AlAsSb barrier, yielding an electron concentration of $5 \times 10^{18} \text{ cm}^{-3}$. Figure 1 also shows the normalized static transmission spectra of the sample obtained by Fourier transform infrared spectroscopy. For this measurement the sample was prepared in a waveguide geometry with several transitions through the stack of QWs. The maximum absorption appears at a wavelength of around 2.1 μm . The absorption spectrum is strongly inhomogeneously broadened due to well width fluctuations at this narrow QW thickness. Since the transition dipole moment for the ISBTs requires a field component along the growth direction, i.e. normal to the samples surface, the sample cannot be used in reflection geometry under normal incidence like a conventional interband saturable absorber.

Instead the sample has to be placed at Brewster angle in the cavity not only to reduce the inserting loss but to obtain a polarization component along the growth axis.

3. Experimental setup and results

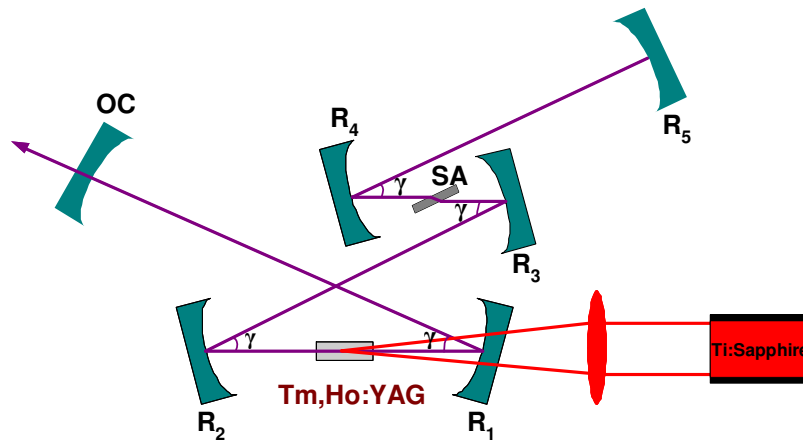


Fig. 2. Schematic of the passively mode-locked Tm,Ho:YAG laser. SA: saturable absorber; OC: output coupler

The schematic laser setup is shown in Fig. 2. The pump source is a wavelength tunable continuous wave Ti:sapphire laser with a maximum output power of 3 W at 785nm, corresponding to the absorption center wavelength of the Tm^{3+} , Ho^{3+} :YAG crystal. The M^2 factor was measured to be about 1.2 and 1.3 in sagittal and tangential plane, respectively. The pump beam was focused into the gain medium by using a lens with a focal length of 145 mm. A 4.9 mm-long 5at.-%- Tm^{3+} , 0.4at.-%- Ho^{3+} :YAG crystal was employed as the gain medium, both sides of which were anti-reflectivity coated at 785 nm (reflectivity <1%) and from 1930 to 2230nm (reflectivity <0.25%). The crystal was water-cooled to 12°C. The laser crystal was placed at the center of the cavity arm formed by mirror R_1 and R_2 , which had the same radii of curvature of 100mm and a reflectivity of 99.9% from 2010 to 2100 nm. In addition, the front surface of mirror R_1 was high transmission coated at 785nm to improve the pump coupling efficiency. Mirror R_3 and R_4 with radii of curvature of 30 mm and 50 mm, respectively, formed another cavity arm providing a focal radius of only 20 μm at the saturable absorber position. To reduce the sensitivity of cavity alignment, the end mirrors R_5 was chosen concave with a radius of curvature of 200 mm. Mirrors R_3 , R_4 and R_5 are all high reflectivity coated from 1930 to 2230nm (reflectivity >99.9%). Four kinds of output couplers (OCs) with different transmissions of 0.5%, 2%, 3% and 5% at 2 μm were used, respectively. The ISBTs $\text{In}_{0.53}\text{Ga}_{0.47}\text{As}/\text{Al}_{0.53}\text{As}_{0.47}\text{Sb}$ MQWs saturable absorber was mounted on a three dimensional translation and rotation stage and inserted in Brewster geometry into the cavity. The distances between OC and R_1 , R_2 and R_3 , R_4 and R_5 were 35cm, 45cm and 45cm, respectively. The whole cavity length is about 1.45m. To compensate the astigmatism induced by the folding mirrors and the saturable absorber placed in Brewster angle, the folding angle γ was 5°. Based on calculations with an ABCD propagation matrix, the laser mode waist radii in the laser crystal were 52 μm and 50 μm in sagittal and tangential planes, respectively, and the beam waist radii at the position of saturable absorber were 20 μm in both sagittal and tangential planes.

Without ISBTs QWs saturable absorber, the Tm,Ho:YAG laser ran in a stable continuous wave regime. Figure 3 shows the average output powers under different output couplers. The threshold absorbed pump powers were 180 mW, 478 mW, 613mW and 725 mW, for the output couplers with transmissions of 0.5%, 2%, 3% and 5%, respectively. The corresponding slope efficiencies η were 22.8%, 41.3%, 41.8% and 42.8%, respectively. A maximum output power of 983 mW was obtained under the absorbed pump power of 2.93 W at the peak

wavelength of 2.097 μm with the output coupler of $T = 2\%$. This corresponds to an optical-optical conversion efficiency of 33.5%. According to the measured slope efficiency η shown in Fig. 3 and the formula $\eta = \eta_q(v_L/v_p)T/(T + L)$ [22], where η_q is the pump quantum efficiency, T is the transmission of the output coupler and L is the intrinsic intracavity loss, v_L and v_p are the laser and pump frequencies, respectively, we can estimate $\eta_q = 1.22$ and $L = 0.53\%$. The pump quantum efficiency is lower than 2 as could be expected from complete cross relaxation case.

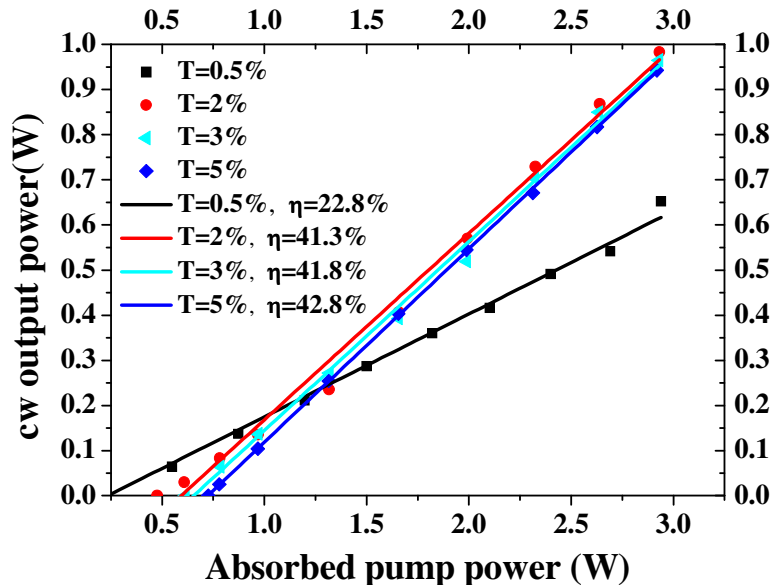


Fig. 3. The average output power versus absorbed pump power for different output couplers

After inserting the $\text{In}_{0.53}\text{Ga}_{0.47}\text{As}/\text{Al}_{0.53}\text{As}_{0.47}\text{Sb}$ MQWs and translating the stage holding the ISBTs QWs saturable absorber, the laser easily turned into passive Q-switching with pulse repetition rate from 10 kHz to 100 kHz, which provided a passive way to obtain Q-switched pulses of several μs in duration at 2 μm . By carefully adjusting the cavity mirrors and position of the saturable absorber, continuous wave mode-locking was achieved with spectra centered at 2.091 μm by using the output couplers of $T = 0.5\%$, 2% and 3% , respectively. However, when the output coupler of $T = 5\%$ was used, continuous wave mode-locking could not happen, which was probably due to the decrease of the intracavity intensity. With a 1 GHz bandwidth digital oscilloscope (DPO, Tektronix Inc.) and a 60 MHz bandwidth extended InGaAs PIN photodiode (G8423, Hamamatsu Inc.), the mode-locked pulse train was monitored to optimize the stability of continuous wave mode-locking. The maximum average output powers of continuous wave mode-locking lasers were 15 mW, 110 mW and 160 mW, respectively, corresponding to the output couplers of $T = 0.5\%$, 2% and 3% . In comparison with continuous wave running regime, the lower output power of continuous wave mode-locking was a result of the additional high non-saturable losses of the saturable absorber (low small signal transition at laser wavelength as shown in Fig. 1). The required high number of QWs in the saturable absorber due to the weak ISBT absorption in every QW is considered as one origin of high non-saturable losses. By using the above mentioned formula in [22] the inserting loss by the saturable absorber is estimated to be about 10% at least, so the output power from the mode-locked laser is expected to be improved by designing the ISBT QWs saturable absorber with higher transmission at 2 μm .

The continuous wave mode-locking was self-starting and could maintain stable over hours if there was not external interruption. The amplitude fluctuation among the pulses is approx.

1%. Figure 4 shows the first beat note of radio frequency (RF) spectrum of the stable continuous wave mode-locking with repetition rate of 106.5 MHz under the absorbed pump power of 2.93 W when the output coupler of $T = 0.5\%$ was employed, which was recorded by a spectrum analyzer with a bandwidth of 3 GHz and a resolution bandwidth of 200 Hz (FS300, ROHDE & SCHWARZ Inc.). The RF spectrum obtained under a span of 2.8 kHz shows a clean peak at the repetition rate of 106.4822 MHz without side peaks, which exactly agrees with the roundtrip time of the cavity and reveals stable continuous wave mode-locking operation of the laser as well as the absence of the Q-switching instabilities. In addition, the wide-span RF measurement indicated the single pulse operation of the Tm,Ho:YAG mode-locked laser, as shown inset of Fig. 4.

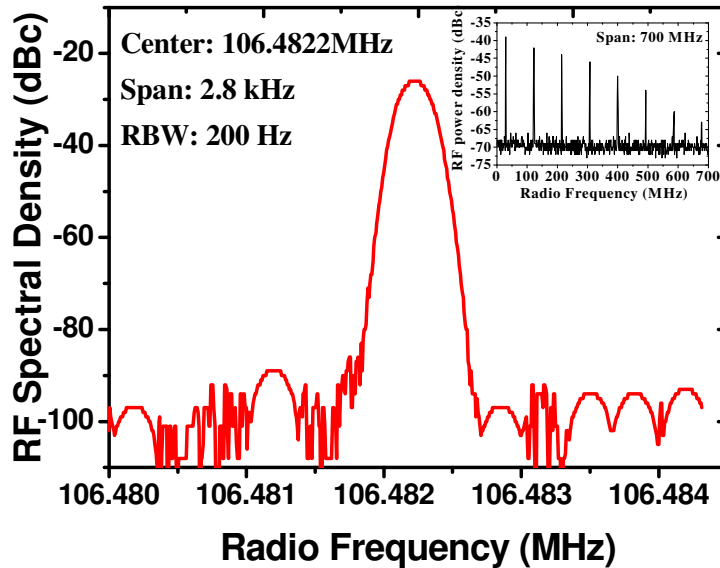


Fig. 4. RF spectrum of continuous wave mode-locked Tm,Ho:YAG laser. RBW: resolution bandwidth.

When the output coupler was $T = 2\%$, the continuous wave mode-locking threshold was about 1.45 W of absorbed pump power, at which 33.5 mW of output power was produced as shown in Fig. 5. The corresponding intracavity fluence on the ISBT's saturable absorber was about $1200 \mu\text{J}/\text{cm}^2$, which demonstrates a high saturation fluence of the saturable absorber due to the weak coupling of the laser polarization to the intersubband transition in the Brewster geometry used. The corresponding slope efficiency of mode-locking operation is only about 6%, which is similar to the case with output coupler of $T = 3\%$.

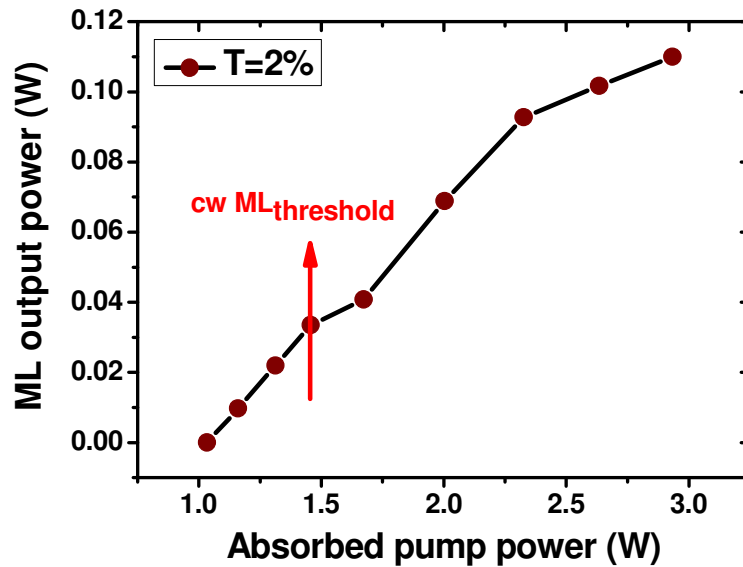


Fig. 5. Power transfer characteristics of the mode-locked Tm,Ho:YAG laser with output coupler of $T = 2\%$.

We employed collinear autocorrelation setup using second harmonic generation with a PPLN doubling crystal to determine the pulse length and Fig. 6 shows the intensity autocorrelation trace recorded at the output power of 110mW, from which the shortest pulse length is deduced to be 60 ps by assuming a Gaussian shaped pulse. The spectrum of the continuous wave mode-locked laser was measured by a laser spectrometer with a resolution bandwidth of 0.4 nm (APE WaveScan, APE Inc.).

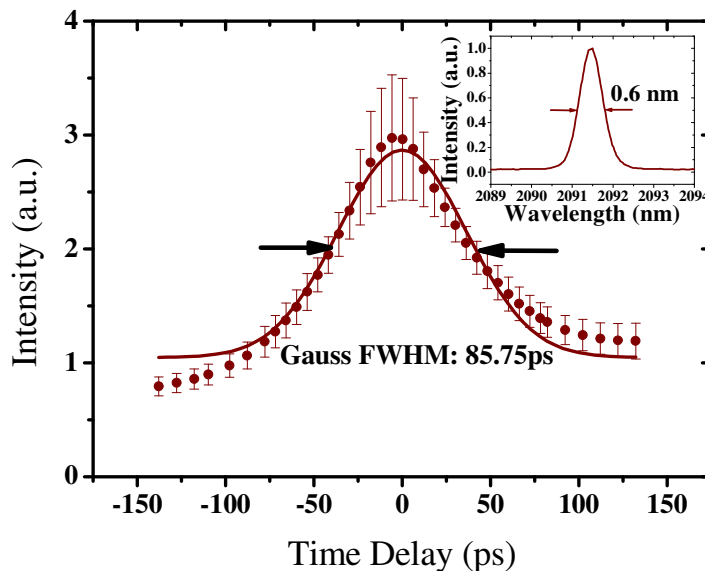


Fig. 6. Envelope of the collinear autocorrelation intensity trace and spectrum of continuous wave mode-locked Tm,Ho:YAG laser

The inset in Fig. 6 shows the spectrum of the continuous wave mode-locked Tm,Ho:YAG laser, and the corresponding spectral width turned out to be around 0.6 nm at the center wavelength of 2.091 μm . It is apparent that the time bandwidth product (TBP) of nearly 2.5 is much larger than the transform limited value of 0.441 for Gaussian shaped pulse, indicating the mode-locked pulse is highly chirped. The origin of the chirp is probably because the intracavity dispersion was not compensated by any means. More recently, A. A. Lagatsky et.al have shown that the intracavity dispersion can apparently affect the mode-locked pulse duration as saturable absorber with faster relaxation time is used [23]. So the pulse length is expected to be shortened by compensating the intracavity dispersion appropriately, especially when crystals with broader gain bandwidth than Tm,Ho:YAG are used, e.g., the tungstate crystals [14,15,23,24] and silicate crystals [25].

4. Conclusion

In conclusion, we have demonstrated a self-starting continuous wave Ti:sapphire laser end-pumped passively mode-locked Tm,Ho:YAG laser at the center wavelength of 2.091 μm utilizing intersubband transitions in $\text{In}_{0.53}\text{Ga}_{0.47}\text{As}/\text{Al}_{0.53}\text{As}_{0.47}\text{Sb}$ quantum wells for the first time. Stable passive mode-locking operation has been obtained with a maximum average output power of 160 mW at a repetition rate of 106.5 MHz. The shortest mode locked pulse is measured to be about 60 ps, which could be further shortened by compensating the intracavity dispersion.

Acknowledgements:

The work was supported by the Ministry of Science, Research and the Arts of Baden-Württemberg. Kejian Yang acknowledges support from the Alexander-von-Humboldt Foundation. We thank Ernst Heumann and Guenter Huber from the University of Hamburg for helpful discussions and for providing the Tm,Ho:YAG crystal.